
Article:
Beranger, G.E., Pisani, D.F., Castel, J. et al. (9 more authors) (2014) Oxytocin Reverses Ovariectomy-Induced Osteopenia and Body Fat Gain. Endocrinology, 155 (4). pp. 1340-1352. ISSN 0013-7227

https://doi.org/10.1210/en.2013-1688

Oxytocin reverses ovariectomy-induced osteopenia and body fat gain

Abbreviated title: Oxytocin controls bone and fat mass

Guillaume E. Beranger[1,2,3], Didier F. Pisani[1,2,3], Julien Castel[4], Mansour Djedaini[1,2,3], Séverine Battaglia[5], Jérôme Amiaud[5], Florian Boukhechba[6], Gérard Ailhaud[1,2,3], Jean-François Michiels[7,8], Dominique Heymann[5], Serge Luquet[4] and Ez-Zoubir Amri[1,2,3*].

[1]Univ. Nice Sophia Antipolis, iBV, UMR 7277, 06100 Nice, France. [2]CNRS, iBV UMR 7277, 06100 Nice, France. [3]Inserm, iBV, U1091, 06100 Nice, France. [4]University of Paris Diderot, Sorbonne Paris Cité, BFA, EAC 4413 CNRS, F-75205 Paris, France. [5]University of Nantes, INSERM, UMR 957, Nantes, Equipe Labellisée Ligue Contre le Cancer 2012, France. [6]Graftys SA, Aix-en-Provence, France. [7]University of Nice Sophia Antipolis, UFR Médecine, Nice, F-06189. [8]Anatomopathology Service, Pasteur Hospital, Centre Hospitalier Universitaire de Nice, Nice, France.

[*]Correspondence should be addressed to EA: Dr. Ez-Zoubir Amri, iBV, Institut de Biologie Valrose, Univ. Nice Sophia Antipolis, Tour Pasteur, UFR Médecine, 28, avenue de Valombrose, 06189 Nice Cedex 2, France

Tel: +33 493 37 70 82; Fax: +33 493 81 70 58; E-mail: amri@unice.fr

Key words: Oxytocin, osteoporosis, intra-abdominal adipose tissue, ovariectomy, menopause

Fundings: This work was supported by CNRS (Centre National de la Recherche Scientifique), Fondation pour la Recherche Médicale, the “Agence Nationale de la Recherche” (ANR).

DISCLOSURE STATEMENT: The authors have nothing to disclose.

5168 words

ABSTRACT

Osteoporosis and overweight/obesity constitute major worldwide public health burdens that are associated with aging. A high proportion of women develop osteoporosis and increased intra-abdominal adiposity after the menopause which leads to bone fractures and metabolic disorders. There is no efficient treatment without major side effects for these two diseases. We previously showed that the administration of oxytocin normalizes ovariectomy-induced osteopenia and bone marrow adiposity in mice. Ovariectomized mice, used as an animal model mimicking menopause, were treated with oxytocin or vehicle. Trabecular bone parameters and fat mass were analyzed using micro-computed tomography. Herein, we show that this effect on trabecular bone parameters was mediated through the restoration of osteoblast/osteoclast cross-talk via the RANKL/OPG axis. Moreover, the daily administration of oxytocin normalized body weight and intra-abdominal fat depots in ovariectomized mice. Intra-abdominal fat mass is more sensitive to oxytocin that subcutaneous fat depots and this inhibitory effect is mediated through inhibition of adipocyte precursor's differentiation with a tendency to lower adipocyte size. Oxytocin treatment did not affect food intake, locomotors activity and energy expenditure, but it did promote a shift in fuel utilization favoring lipid oxidation. In addition, the decrease in fat mass resulted from the inhibition of the adipose precursor's differentiation. Thus, oxytocin constitutes an effective strategy for targeting osteopenia, overweight and fat mass redistribution in a mouse model mimicking the menopause without any detrimental effects.

INTRODUCTION

Human life expectancy has increased continuously in industrialized countries. Aging is associated with immunosenescence, a decrease in hormonal secretion, lean mass and bone mass, and an increase in fat accumulation. Body weight gain and fat mass redistribution toward the intra-abdominal compartment represent a major worldwide public health problem, as a large proportion of the adult population is at risk of becoming overweight/obese and developing associated diseases (1,2). Osteoporosis also represents a major health threat as it already affects 40% of white postmenopausal women and is expected to increase concomitantly with life span in the coming years. Post-menopausal osteoporosis is responsible for a dramatic increase in fractures which lead to loss of mobility and autonomy, and more importantly to an increase in mortality of up to 20% one year afterwards due to complications (3).

The menopause is a critical period of a woman's life, which is characterized by decreased ovarian hormone production due to age and during which weight gain and the onset or worsening of obesity and osteoporosis are favored (4-6). Such weight gain preferentially affects the abdominal fat depot associated with a transition of body distribution from a gynoid to an android type (7,8). This shift in fat mass distribution favors the development of insulin resistance and its clinical outcomes leading to increased cardiovascular risks and cancer among other diseases (9). Estrogen therapy has been shown to normalize intra-abdominal fat mass and bone resorption in both animals and humans (10-12). However, the side effects of estrogens on non-fat organs hamper the possibility of using this hormone therapeutically as many controversial studies have been reported, in which hormonal replacement therapy may lead to cardiovascular diseases and breast cancer (13,14).

Recent studies have shown that obesity and osteoporosis share common traits(15-18): i) both diseases are affected by genetic and environmental factors, or the interaction between them; ii) normal aging is associated with a high incidence of both osteoporosis and bone marrow adiposity; iii) bone remodeling and adiposity are both regulated through the hypothalamus and sympathetic nervous system; iv) adipocytes and osteoblasts arise from a common progenitor, the mesenchymal stem cell; v) adipose tissue and skeleton are endocrine organs; vi) pathophysiological relevance of adipose tissue in

bone integrity lies in the participation of adipokines in bone remodeling, while the skeleton has effects on body weight control and glucose homeostasis through the actions of bone-derived factors such as osteocalcin and osteopontin (19-22). However, several studies have suggested that obesity is able to protect postmenopausal women from osteoporosis (23,24). This would be due to the impact of being overweight on osteocyte signaling through mechanical loading. It is now accepted that there is a negative correlation between bone and body fat mass suggesting that obesity represents a risk for osteoporosis (17,25,26). Furthermore, recent reports suggested a detrimental effect of intra-abdominal adipose tissue on bone mineral density in premenopausal obese women (27-30). Thus, there is an active cross-talk between adipose tissue and the skeleton which constitutes a homeostatic feedback system with adipokines and molecules secreted by osteoblasts and osteoclasts (20).

Based on the linkage between osteoporosis and intra-abdominal adiposity, the inverse relationship that exists between osteogenesis and adipogenesis, controlling the fine balance between the two pathways, is of clear therapeutic significance (31). In our previous work, we showed that oxytocin (OT) inhibited adipocyte and stimulated osteoblast differentiation. Plasma OT levels were lower in ovariectomized (OVX) mice and rats compared to sham-operated controls and OT plasma levels were significantly lower in postmenopausal women who developed osteoporosis than in their healthy counterparts (32).

In this study we show that, in OVX mice, OT administration reverses osteopenia and improves fat mass distribution at the onset and after establishment of both disorder phenotypes. The peripheral effect of OT is mediated through an osteoblast/osteoclast cross-talk and an inhibitory effect on the adipocyte precursor's differentiation. Furthermore, the effects of OT on fat mass, body weight loss and decrease of intra-abdominal fat depots are observed with no change in food intake and OT induces a shift in favor of lipid consumption at the expense of carbohydrates. Collectively, these results indicate that administration of OT holds promise as a preventive as well as a curative therapy for osteoporosis and weight gain/fat mass redistribution.

MATERIALS AND METHODS

Animals

The experiments were conducted in accordance with the French and European regulations for the care and use of research animals and were approved by the local experimentation committee. Animals were maintained under constant temperature (21 ± 2°C) and 12:12-hour light-dark cycles, with ad libitum access to standard chow diet and water. Ten-week-old C57Bl/6J mice were subjected either to bilateral ovariectomies from the dorsal approach or to sham surgery in which the ovaries were exteriorized but replaced intact by Charles River Laboratories. 2 or 8 weeks after the ovariectomy or sham surgery, groups of mice (n= 6 to 12) were injected daily intra-peritoneally with vehicle (Ve) or different doses of OT (0.1 or 1 mg/kg, Bachem #H2510) for 8 weeks unless otherwise indicated.

Plasma measurements

Leptin (Assay Pro), Procollagen I N-Terminal propeptide (PINP, USCN) or Cross Linked C-Telopeptide of Type I Collagen (CTXI, USCN) plasma levels were measured using an ELISA kit as per the manufacturer's instructions.

Energy expenditure, food intake and locomotors activity.

Mice were analyzed for whole energy expenditure, oxygen consumption and carbon dioxide production, respiratory quotient (vCO_2/vO_2), food intake and locomotors activity (counts/hour) using calorimetric equipment (Labmaster). Activity was recorded using an infrared light beam-based locomotion monitoring system. Individually housed mice were acclimatized to the chambers for 48 hours before experimental measurements and the first day of data acquisition were systematically removed from the final analysis. Data analysis was performed using O_2 consumed (ml/h), CO_2 production (ml/h), and energy expenditure (kcal/h) which were subsequently expressed as a function of whole lean body mass measured through NMR. Data was expressed as an average of the 4 last days of a total of 5 days baseline acquired in the system. The effect of OT injections was conducted as follows: a first analysis was performed after 2 weeks of treatment and a second after 9 weeks. As consistent changes were observed at the onset of the dark cycle, average RER values were calculated systematically using the same 4-hour period during the dark cycle.

Micro-computed Tomography

Trabecular bone microarchitecture of the distal femoral metaphysis was analyzed using the high-resolution SkyScan-1076 X-ray micro-computed tomography system (SkyScan). Femora were scanned after necropsy using the same parameters: 9 µm of voxel size, 49 kV, 0.5 mm thick aluminium filter, 0.5° of rotation step. Calculation of femur trabecular bone parameters (Bone Volume / Total Volume: BV/TV) following 3-D morphometric parameters (Bone ASBMR nomenclature (33,34)) were performed on secondary spongiosa: 100 slides of microCT (0.9 mm of height) starting at 0.45 mm from the lower part of the distal growth plate. With such parameters, we included almost all the trabeculae from the distal metaphysis in our mice, excluding the primary spongiosa and the cortical bone. For vertebrae analysis, the 4th lumbar vertebra was scanned after necropsy using the same settings as described previously and trabecular parameters were analyzed on a 1.8 mm height region of interest within the vertebral body.

Adipose tissue quantification was carried out using a SkyScan-1178 X-ray micro-computed tomography system. Mice were anaesthetized and scanned using the same parameters: 104 µm of voxel size, 49 kV, 0.5 mm thick aluminum filter, 0.9° of rotation step. Total adipose tissue volume was determined between the lumbar vertebra 1 (L1) and the caudal vertebra 4 (C4), whereas intra-abdominal and subcutaneous adipose tissues areas were measured on one section at the lumbar 5 (L5) level. Subcutaneous and intra-abdominal adipose tissue is based on the delimitation of region of Interest (ROI) after 3D reconstruction of scanned images as described in (35). 3-D reconstructions and analysis of bone parameters and adipose tissue areas or volumes were performed using NRecon and CTAn software (Skyscan).

Histology.

Tracp and Osterix staining. Femora were fixed in Phosphate Buffered Formaldehyde and decalcified in EDTA solution over 72 hours using a temperature controlled microwave oven to accelerate the decalcification process (KOS, MM France) before being embedded in paraffin. Transversal 3 µm thick sections were stained for tartrate-resistant acid phosphatase (TRACP), after 1-hour incubation in a solution containing 1 mg/mL naphthol AS-TR phosphate, 60 mM NNdimethylformamide, 100 mM Na tartrate, and 1 mg/mL Fast red TR salt solution and

counterstained with hematoxylin. Osterix staining was performed on decalcified femora sections using an antibody from Abcam. Osteoblast number and osteoclast surface were quantified in a region of interest including both primary and secondary spongiosa. These quantifications have been performed on ten 10X-fields per section, one sample per animal and 12 mice per group.

Adipocyte size determination. Adipose tissues were fixed in Phosphate Buffered Formaldehyde, embedded in paraffin and 4 µm thick sections were stained with hematoxylin/eosin/safran. Adipocyte size was measured using ImageJ software. At least 40 adipocytes per section were measured and 8-12 samples were analyzed per group.

Isolation and analysis of RNA.

Total RNA was extracted using a TRI-Reagent (Euromedex) kit as per the manufacturer's instructions. Two micrograms of total RNA, digested with Dnase I (Promega), were subjected to reverse transcription-polymerase chain reaction (RT-PCR) analysis as described previously (32). The oligonucleotide sequences, designed using Primer Express software, are shown in Supplemental Table 1.

Cell culture.

Primary osteoclast culture and co-culture. Bone marrow-derived primary monocytes were isolated from mouse long bones. Bone marrow cells were collected by flushing tibial and femoral shafts. Monocytes were then isolated using the EasySep® Mouse Monocyte Enrichment Kit (Stem Cells Technologies) according to the manufacturer’s instructions. Briefly, mouse monocytes were enriched from mouse bone marrow by depletion of T cells, B cells, NK cells, dendritic cells, progenitors, granuloctyes and red blood cells. For osteoclastic differentiation, freshly isolated enriched monocytes were seeded at 25,000 cells/cm^2 and cultured for 7 days in the presence of α-MEM supplemented with 10% FCS, 20 ng/ml M-CSF (Peprotech) and 20 nM RANKL. For co-culture experiments, monocytes were seeded at a density of 25,000 cells/cm^2 with ST2 cells seeded at 20,000 cells/cm^2 in α-MEM supplemented with 10% FCS, 10^{-8} M 1α,25-Dihydroxyvitamin D3 and 10^{-7} M dexamethasone for 7 days. 300 nM OT was added daily to the cell culture medium.

Primary adipocyte culture. Stromal-vascular fraction cells were isolated and induced to differentiate in the presence of DMEM containing 10% FCS, 0.5µM dexamethasone, 0.5 mM isobutylmethylxanthine, 170 nM insulin and 1 µM Rosiglitazone. Dexamethasone and isobutylmethylxanthine were omitted 2 days later and cells were maintained for 7-10 days in the presence of 170 nM insulin and 1 µM Rosiglitazone. 30 or 100 nM OT was added daily to the cell culture medium.

Tracp staining and osteoclast quantification

Tracp activity was detected using the leukocyte acid phosphatase kit from Sigma-Aldrich as per the manufacturer's instructions. Tracp positive cells with at least 3 nuclei were counted as osteoclasts. For co-culture experiments, Tracp positive areas were quantified using ImageJ software.

Statistical analyses

Data is expressed as mean values ± SEM and was analyzed using the 2-tailed Student's t -test. Differences were considered statistically significant at $p \leq 0.05$. ANOVA and post-hoc Tukey-Kramer multiple comparison's test for the data involving the 2 doses of oxytocin were performed.

RESULTS

Oxytocin normalizes bone parameters and fat mass gain in ovariectomized mice.

Our aim was to determine whether OT treatment is efficient to normalize osteopenia and body weight gain. Ovariectomized (OVX) or control (Sham) mice received OT or vehicle (Ve) over 8 weeks according to the two protocols described in Figure 1a and 1b. In the first protocol, we treated mice 2 weeks post-surgery which corresponded to the onset of bone and fat mass disorders; such treatment was considered as a preventive therapy. Of note, this time point corresponds to a high bone turnover as described previously (36). Indeed, a significant increase of Tracp staining and Tracp mRNA expression is observed in long bones of OVX mice 2 weeks after ovariectomy (Supplemental Figure 1). In the second protocol we treated mice 8 weeks post-surgery at a stage where mice developed osteopenia and a net increase in intra-abdominal fat mass; such treatment represented a potential curative therapy. Body weight was monitored during the treatment and trabecular bone

parameters from distal femoral metaphysis and fat mass were analyzed using micro-computed tomography (Micro-CT) at the end of the experiments. Using the first protocol, a daily injection of OT (1 mg/kg) was able to normalize ovariectomy-induced osteopenia (Figure 1c and Table 1) in agreement with our previous data (32). The BV/TV ratio, trabecular spacing and number were normalized upon OT treatment of OVX mice. In order to determine whether a continuous daily treatment was necessary to restore bone parameters, OVX mice were either injected daily with 1mg/kg OT during the first 4 weeks and received vehicle during the last 4 weeks (short treatment), or they were treated twice a week, vehicle was injected the other days of the week, over 8 weeks (Figure 1a). Micro-CT analysis shows that the BV/TV and the trabecular number of mice that received OT twice a week were restored to the levels of Sham mice, whereas mice that received OT during the first 4 weeks only (short treatment) did not recover the normal parameters (Figure 1c and Table 1). In parallel, we also analyzed by micro-CT the trabecular parameters of the 4th lumbar vertebra. Whereas ovariectomy induces a decrease in bone volume within the vertebral body, OT treatment does not rescue these parameters (Supplemental Table 2). Bone resorption (CTX-I) and formation (PINP) plasma marker levels were measured and for which no significant changes was observed except for PINP which is induced in OVX mice upon OT treatment but only in the late treatment protocol (Figure 2a-d). These results demonstrate that the restoration of bone trabecular parameters by OT is not a consequence of either excessive anabolic activity or a dysregulation of bone turnover.

Regarding fat mass, it is well known that OVX mice gain body weight after surgery and exhibit increased intra-abdominal fat mass. Daily OT injections (1 mg/kg) significantly reduced mice body weight under each protocol (Figure 1e and 1f). In contrast with the effects on bone parameters, the OT treatment twice a week was less effective in decreasing body weight (Figure 1e). Interestingly, mice receiving OT during the first 4 weeks only (short treatment) immediately gained weight once the OT treatment was completed and returned to the level of OVX-Ve treated mice within 4 weeks (Figure 1e). With the second protocol, OVX-OT treated mice exhibited a significant lower body weight compared to OVX-Ve treated mice after 8 weeks of treatment with the two doses used (0.1 mg/kg and 1 mg/kg, Figure 1f). Of note, OT did not significantly affect the body weight of Sham mice using

either protocol (Figure 1f). Micro-CT quantification of the adipose tissue volume between vertebrae L1 and C4 (Figure 1g and 1h) showed that daily injections of 1 mg/kg OT for 8 weeks were able to reduce significantly the adipose tissue volume of OVX mice. The short treatment was not efficient whereas injections twice a week enabled a weak but not significant adipose tissue volume reduction (Figure 1g). Furthermore, OT restored adipose tissue volume significantly for the 1 mg/kg dose (Figure 1h). These variations in adipose tissue volume and body weight correlated with the circulating levels of leptin, a marker of fat mass, which decreased upon OT treatment (Figure 2e and 2f). Body composition analysis showed that the difference in body weight was due to a decrease in fat mass weight, whereas lean mass was not affected by OT treatment (Supplemental Figure 2). In agreement with our previous work (32), OT treatment of OVX mice normalized bone adiposity and fabp4 mRNA expression (Supplemental Figure 3a and b).

OT treatment restores osteoblast/osteoclast coupling in vivo and in vitro through an increase of RANKL/OPG ratio.

Histological analyses on decalcified femora sections using Tracp and Osterix staining revealed that both osteoclast and osteoblast numbers decreased dramatically in OVX mice. OT treatment of OVX mice partially restored the osteoclast number (Tracp-positive areas, Figure 3a) and totally normalized the osteoblast number (Osterix-positive cells, Figure 3c) in long bones, whereas there was no significant effect on Sham-OT treated mice. In agreement with these observations a significant decrease in the expression of osteoclast (Tracp, Atp6v0a3 and *Integrinβ3*) and osteoblast (osteocalcin and *Col1α1*) specific markers in OVX compared to Sham mice bones was observed (Figure 3b and 3d). OT treatment of OVX mice induced a partial restoration in the expression of osteoclast markers (Figure 3b) and a complete restoration in that of osteoblast markers (Figure 3d). Furthermore, TNFα mRNA expression and RANKL/OPG mRNA ratio were increased in OVX-OT treated mice (Figure 3e and 3f). Of note, OT treatment did not alter the expression of bone remodeling markers in Sham mice.

We next aimed to know whether OT induces osteoclastogenesis in OVX mice through a direct effect, since both osteoblasts and osteoclasts express the OT receptor (OTR). Monocytes isolated from

bone marrow of OVX mice were induced to differentiate into osteoclasts either alone (Figure 4a and 4b) or in co-culture in the presence of ST2 mesenchymal stromal cells (Figure 4c-f). OT treatment did not significantly affect monocyte differentiation as measured by Tracp and Calcitonin Receptor (CTR) mRNA levels (Figure 4a) and TRACP staining of multinucleated cells (Figure 4b). When OVX bone marrow derived monocytes were differentiated using the co-culture protocol, a strong increase in the expression of both Tracp and CTR mRNAs was observed upon OT treatment (Figure 4c). Furthermore, OT treatment triggered a 2.5-fold increase in the Tracp-positive areas (Figure 4d) as well as a 3.5-fold increase in the RANKL/OPG mRNA ratio (Figure 4e). The Tracp-positive areas induced by OT in co-culture experiments decreased dramatically in the presence of increasing amounts of OPG, the decoy receptor for RANKL, thus inhibiting osteoclast differentiation (Figure 4f). These observations demonstrate that OT induces osteoclastogenesis through the induction of the RANKL/OPG ratio by mesenchymal cells.

Effects of oxytocin on metabolic parameters.

In order to gain insights into the role played by OT in the regulation of fat mass, we next investigated the effect of OT treatment on overall energy metabolism. Mice were treated according to the late treatment protocol described in Figure 1b and were monitored in metabolic cages over 5 days. Two periods of analyses were performed, i.e. at 2 weeks after the beginning and at the end of the OT treatment (Figure 5a). Food intake measurements showed that OVX mice were not hyperphagic and that OT did not affect this parameter in both OVX and Sham mice (Figure 5b). Moreover, a more detailed analysis of food intake on a short term period does not evidence any differences following OVX or OT treatment (Supplemental Figure 4a and 4b). However, if we focus on meal pattern, we observe a significant decrease in meal size and duration in OVX-OT treated mice (Supplemental Figure 4c and 4d). OVX mice exhibited reduced locomotors activity (Figure 5c) and energy expenditure during the night period compared to Sham mice regardless of OT treatment (Figure 5d). Interestingly, even if OVX-OT treated mice lost body weight and fat mass, daily OT injections did not promote an increase in physical activity or energy expenditure (Figure 5c and 5d).

Under a situation where food intake is similar for OT or vehicle treated OVX and Sham mice (Figure 5b), we sought out a physiological explanation for OT-induced body fat mass loss. We found that the respiratory exchange ratio was significantly lower in OVX-OT compared to OVX-Ve mice (Figure 5e) indicating that a change in fuel utilization had occurred which favored a higher rate of lipid oxidation. Altogether, these observations suggested that OT treated mice used more lipids as energy source than vehicle treated controls which explains the beneficial effects of OT on adipose tissue weight loss. Furthermore, plasma and liver triglyceride as well as plasma glycerol levels were not affected by the OT treatment (Supplemental Figure 5).

Glucose tolerance tests showed that glucose tolerance was not affected by OT treatment (Supplemental Figure 6a and 6c). Interestingly, insulin secretion was in a tendency of normalization (Supplemental Figure 6b and 6d), suggesting that OT might protect against ovariectomy-induced insulin resistance consistent with the normalization of body fat mass. We then measured the circulating levels of osteocalcin and its undercarboxylated form (Glu-OC). Glu-OC is considered as a hormone and exerts metabolic functions on different targets such as pancreatic β-cells and fat cells (19). As shown, in Supplemental Figure 7a and 7b, the Glu/Gla ratio was not altered following ovariectomy and OT treatment thus indicating that osteocalcin is not involved in OT impact on adipose tissue and pancreas.

Oxytocin reduces both intra-abdominal and subcutaneous adipose tissue mass without affecting adipocyte cell size.

We quantified the subcutaneous and the intra-abdominal adipose tissue depots by measuring their respective areas on a transversal section at the 5th lumbar vertebra level. Ovariectomy was associated with an increase in both fat depots (Figure 6a and 6d). However, the intra-abdominal fat areas were increased at a higher extent (6-fold vs Sham mice, Figure 5a) compared to subcutaneous fat areas (2-fold vs Sham mice, Figure 6d). Daily OT injections (1 mg/kg) in OVX mice were able to restore the areas of subcutaneous and intra-abdominal adipose tissues to those of Sham mice under both the early and late treatment protocols (Figure 6a and 6d, and Supplemental Figure 8a and 8b). Moreover,

treatment with 0.1 mg/kg OT displayed a significant effect on the intra-abdominal compartment suggesting that this fat depot is more sensitive to OT treatment than the subcutaneous adipose tissue. The two other treatments used (OT injections twice a week, short treatment), were inefficient (Supplemental Figure 8a and 8b).

Histological analyses of intra-abdominal and subcutaneous fat depots showed that ovariectomy induced adipocytes hypertrophy in both depots (Figure 6b and 6e), as adipocyte size increased with a trend toward a greater proportion of larger adipocytes (Figure 6c and 6f). OT treatment did not significantly affect adipocyte size in subcutaneous and intra-abdominal adipose tissue depots although there was a tendency towards a decrease in cell diameter (Figure 6b and 6e). These observations suggest that OT treatment led to a reduction of fat mass mainly through a decrease in the formation of new adipocytes rather than a decrease or a blockage in adipocyte hypertrophy.

In order to distinguish between a peripheral and a central effect of OT that could be involved in the decrease in fat mass, we analyzed in vitro the direct effect of OT on the differentiation of mouse adipose precursor cells. For that purpose, stromal-vascular fraction cells were isolated from subcutaneous adipose depots of OVX mice and induced to differentiate into adipocytes in the presence or the absence of 30 or 100 nM OT. The yield of differentiation was then assessed morphological analysis (Figure 7a) and real-time PCR analysis of adipocyte specific markers (Figure 7b). We observed a strong decrease in the number of lipid droplet-containing cells isolated from subcutaneous depots and a parallel decrease in the expression of adipocyte markers such as adiponectin, fabp4 and adipsin. These observations demonstrate that OT can directly target and inhibit differentiation of mouse adipose precursor cells. Together with the previous results which demonstrated that fat mass reduction in vivo following OT treatment is related to a reduction in adipocyte cell numbers, these data suggest that the propensity to acquire new fat cells from precursor cells in vivo is reduced upon OT treatment of OVX mice.

DISCUSSION

Our study demonstrates that a single hormone, oxytocin, is able to normalize osteopenia and intra-abdominal adiposity in ovariectomized mice, an animal model mimicking the menopause. Osteoporosis and overweight/obesity are two major global health problems with an increasing prevalence and a high impact on mortality and morbidity. The menopause, corresponding to the cessation of ovarian estrogen production, is associated with bone loss and increased intra-abdominal adiposity. In contrast to previous contentions, obesity does not protect against osteoporosis and recent studies have suggested that increased intra-abdominal fat has detrimental effects on bone health (28,30). Patients with increased fat accumulation in the abdominal area, even in the absence of obesity features (BMI < 30), have a higher risk of developing diabetes and cardiovascular diseases.

So far, there is no efficient treatment free from side effects that is able to restore bone health and to decrease intra-abdominal adiposity and the associated diseases such as cardiovascular dysfunctions and type 2 diabetes. Hormonal replacement therapy is beneficial for bone and fat mass normalization; however this therapy increases the risks of developing breast cancer and cardiovascular diseases (37). Current therapies for osteoporosis mainly consist of anti-resorptive treatments, such as bisphosphonates, estrogen, selective estrogen receptor modulators, calcitonin and a monoclonal antibody against RANKL. The only currently available anabolic treatment for osteoporosis is parathyroid hormone (PTH), but this treatment has a time-limited “anabolic window” and is far from being considered as a “gold standard” therapy. Indeed on a long term basis, PTH treatment enables an increase in bone resorption and a higher bone remodeling turnover that allowed the need to be given in association with a bisphosphonate treatment in an alternative manner (37,38).Thus, OT seems to be a promising candidate for treating osteoporosis, as it was previously described as an anabolic hormone in vivo and an anti-resorptive agent in vitro (this study and (32,39)). Furthermore, we describe in this work that OT, in an osteoporotic context, restores bone coupling in vivo establishing a new steady-state which contrasts with PTH treatment (38). Of note, treatment of osteoporotic patients with PTH led to a relative normalization of bones with some side effects but did not normalize body weight or fat mass distribution. This work was performed using OVX mouse as a model for post-menopausal osteoporosis which is extensively used to investigate the effects of different treatments such as PTH

and bisphosphonates. However, some discrepancies exist between the pathophysiological processes of osteoporosis in women compared to the OVX mouse. Indeed, OT has the ability to restore bone homeostasis when applied either 2 weeks post-OVX, when bone turnover and resorption are induced, or 8 weeks post-OVX, when both osteoblast and osteoclast activities are decreased, leading us to propose that OT has a highly interesting therapeutic potential in the context of osteoporosis.

Transcription of the OT and OTR genes is under the control of estrogens (40). Therefore, as estrogen level is decreased in OVX mice and rats as well as in postmenopausal women, OT levels are lowered as a consequence (32). Our previous data strongly suggested that hypogonadal-induced bone loss and fat mass increase were both linked to low OT circulating levels, and that restoring OT levels could therefore reverse osteopenia and fat mass increase. Furthermore, OTR-deficient mice exhibit disorders in several aspects of social behavior, bone defects and develop late-onset obesity (39,41-44). Our present data clearly shows that OT is able to restore bone microarchitecture and to prevent the development of intra-abdominal fat mass in ovariectomized mice, both at the onset and later when the disorders are well established. Interestingly, it has been recently shown in vivo that the expression of osteoblastic OTR, by contrast to osteoclastic OTR, was required for the beneficial effects of OT (45). Herein, we show that the beneficial effect of OT on bone microarchitecture is mediated through an induction of bone modeling. This event is then associated to an increase in bone remodeling, due to the non-direct rescue of osteoclastogenesis through the induction of RANKL/OPG ratio by mesenchymal cells. Altogether, the tight regulation of osteoblast and osteoclast activities by OT leads to a new homeostasis within bone tissue.

As OT affects osteoblast/adipocyte balance at the expense of adipocytes, we hypothesized that OT treatment of OVX mice could lead to a net prevention of increased body weight and fat mass. Recent reports have shown that OT controls body weight and fat mass content in mice under a high fat diet through a decreased food intake (46-49). These observations are in contrast with our data as no difference in food intake following OT treatment could be measured. In our hands mice were fed a standard chow and not a high fat diet which might explain the difference in feeding behavior. Recent data showed that OT reduces body weight in humans and improves insulin secretion in high fat diet

treated mice (50). Our data shows that OT did not affect food intake and energy expenditure, in either OVX or Sham control mice but it did improve insulin sensitivity and promoted a shift in fuel utilization. This change in RER demonstrated that fat oxidation was favored as an energy source, as RER usually ranges from 0.7 (pure fat oxidation) up to 1.0 (pure carbohydrate oxidation). Furthermore, OT did not significantly affect the adipocyte size, and data from in vitro experiments supports the inhibitory effect of OT on adipocyte differentiation of precursor cells. The effects of OT were more efficient on intra-abdominal compared to subcutaneous fat mass that could be due at least in part to the intrinsic differences in adipocyte precursors from different adipose tissue depots recently reported (51). Altogether we attributed the beneficial action of OT on body fat gain to the inhibition of adipogenesis in combination with an increase in the peripheral utilization of lipid substrate. We calculated that OT treatment resulted in a differential accumulation of adipose mass of roughly 3 g (7.5 g - 4.5 g) which corresponded to approximately 21 kcal over the 70 days of treatment, assuming that 7 kcal is consumed per g of fat mass. The body weight loss is therefore the result of a daily differential in energy of about 0.3 kcal, which represented ~2% of the 14 kcal total daily calorific intake. This calculation illustrates how a small differential in energy balance is sufficient for a dramatic output on adiposity (52). We believe that free fatty acids from adipose tissue were the main source of the lipids sustaining the shift in RER, since hepatic triglycerides did not show any difference between OT-treated and vehicle-treated animals.

The crosstalk between bone and energy metabolism has been clearly evidenced in the last years through the investigations on the role of leptin, osteocalcin and other molecules (53). The complexity of the bone phenotype of leptin signaling deficient mouse models highlights the intricacy of the crosstalk between these 2 organs. In the same manner, we identified in this work differential effect of OT on cortical and trabecular bone parameters. Of note, the absence of variation in the levels of undercarboxylated osteocalcin in our mice excludes, at least in part, this pathway for a connection between bone and fat in OT-treated mice. However, we do not exclude the involvement of other molecules. Altogether these observations indicate that the impact of OT on bone and adipose tissues

involve other players such as circulating leptin levels and/or mechanical loading in the normalization of osteopenia and body weight.

In conclusion, our data clearly indicates that administration of OT holds promise as a preventive therapy and may help to reverse both osteoporosis and fat mass increase. This may represent the first therapy targeting these two diseases linked to aging and their associated pathologies such as diabetes and cardiovascular disorders.

ACKNOWLEDGEMENTS

We are grateful to Pr. Dominique Langin for helpful discussions. This work was supported by CNRS (Centre National de la Recherche Scientifique), Fondation pour la Recherche Médicale (grant DVO20081013470) and the Conseil Général des Alpes Maritimes. G.E.B. was supported by "CNRS service Partenariat et Valorisation" and by "Agence Nationale de la Recherche". S.L. was supported by an ATIP grant from CNRS, an equipment grant from the Région Île-de-France, an equipment grant from the University Paris Diderot-Paris 7, a research fellowship from "Société Francophone du Diabète-Lilly" and a grant from the "Agence Nationale de la Recherche" ANR-09-BLAN-0267-02. We would like to express our gratitude to Denis Mestivier, (Université Paris Diderot, Sorbonne Paris Cité, Institut Jacques Monod, Paris, France) for precious input in meal ultrastructure analysis. We acknowledge the Functional & Physiological Exploration Platform at the "Biologie Fonctionnelle et Adaptative" Unit, University of Paris Diderot, for metabolic analysis. The authors declare that they have no competing interests.

REFERENCES

1. Pischon T, Boeing H, Hoffmann K, Bergmann M, Schulze MB, Overvad K, van der Schouw YT, Spencer E, Moons KG, Tjonneland A, Halkjaer J, Jensen MK, Stegger J, Clavel-Chapelon F, Boutron-Ruault MC, Chajes V, Linseisen J, Kaaks R, Trichopoulou A, Trichopoulos D, Bamia C, Sieri S, Palli D, Tumino R, Vineis P, Panico S, Peeters PH, May AM, Bueno-de-Mesquita HB, van Duijnhoven FJ, Hallmans G, Weinehall L, Manjer J,

Hedblad B, Lund E, Agudo A, Arriola L, Barricarte A, Navarro C, Martinez C, Quiros JR, Key T, Bingham S, Khaw KT, Boffetta P, Jenab M, Ferrari P, Riboli E. General and abdominal adiposity and risk of death in Europe. N Engl J Med. 2008;359(20):2105-2120.

2. Despres JP, Lemieux I. Abdominal obesity and metabolic syndrome. Nature. 2006;444(7121):881-887.

3. Rachner TD, Khosla S, Hofbauer LC. Osteoporosis: now and the future. Lancet. 2011;377(9773):1276-1287.

4. Augoulea A, Mastorakos G, Lambrinoudaki I, Christodoulakos G, Creatsas G. Role of postmenopausal hormone replacement therapy on body fat gain and leptin levels. Gynecol Endocrinol. 2005;20(4):227-235.

5. Garaulet M, Perez-Llamas F, Baraza JC, Garcia-Prieto MD, Fardy PS, Tebar FJ, Zamora S. Body fat distribution in pre-and post-menopausal women: metabolic and anthropometric variables. J Nutr Health Aging. 2002;6(2):123-126.

6. Wing RR, Matthews KA, Kuller LH, Meilahn EN, Plantinga PL. Weight gain at the time of menopause. Arch Intern Med. 1991;151(1):97-102.

7. Morris E, Currie H. Obesity in menopausal women: more than you might think. Menopause Int. 2010;16(3):97.

8. Tchernof A, Desmeules A, Richard C, Laberge P, Daris M, Mailloux J, Rheaume C, Dupont P. Ovarian hormone status and abdominal visceral adipose tissue metabolism. J Clin Endocrinol Metab. 2004;89(7):3425-3430.

9. Mendelsohn ME, Karas RH. Molecular and cellular basis of cardiovascular gender differences. Science. 2005;308(5728):1583-1587.

10. Andersson N, Islander U, Egecioglu E, Lof E, Swanson C, Moverare-Skrtic S, Sjogren K, Lindberg MK, Carlsten H, Ohlsson C. Investigation of central versus peripheral effects of estradiol in ovariectomized mice. J Endocrinol. 2005;187(2):303-309.

11. Jensen LB, Vestergaard P, Hermann AP, Gram J, Eiken P, Abrahamsen B, Brot C, Kolthoff N, Sorensen OH, Beck-Nielsen H, Nielsen SP, Charles P, Mosekilde L. Hormone replacement therapy dissociates fat mass and bone mass, and tends to reduce weight gain in early postmenopausal women: a randomized controlled 5-year clinical trial of the Danish Osteoporosis Prevention Study. J Bone Miner Res. 2003;18(2):333-342.

12. Weigt C, Hertrampf T, Zoth N, Fritzemeier KH, Diel P. Impact of estradiol, ER subtype specific agonists and genistein on energy homeostasis in a rat model of nutrition induced obesity. Mol Cell Endocrinol. 2012;351(2):227-238.

13. Vickers MR, MacLennan AH, Lawton B, Ford D, Martin J, Meredith SK, DeStavola BL, Rose S, Dowell A, Wilkes HC, Darbyshire JH, Meade TW. Main morbidities recorded in the women's international study of long duration oestrogen after menopause (WISDOM): a

randomised controlled trial of hormone replacement therapy in postmenopausal women. Bmj. 2007;335(7613):239.

14. Alessandri N, Piccioni MG, Isabelli V, Alessandri G, Di Matteo A, Padovani D, Rondoni G, Camardella B, Parlapiano C. Morphological and functional changes of cardiovascular system in postmenopausal women. Eur Rev Med Pharmacol Sci. 2007;11(2):107-117.

15. Reid IR. Relationships between fat and bone. Osteoporos Int. 2008;19(5):595-606.

16. Shapses SA, Riedt CS. Bone, body weight, and weight reduction: what are the concerns? J Nutr. 2006;136(6):1453-1456.

17. Zhao LJ, Jiang H, Papasian CJ, Maulik D, Drees B, Hamilton J, Deng HW. Correlation of obesity and osteoporosis: effect of fat mass on the determination of osteoporosis. J Bone Miner Res. 2008;23(1):17-29.

18. Rosen CJ, Bouxsein ML. Mechanisms of disease: is osteoporosis the obesity of bone? Nat Clin Pract Rheumatol. 2006;2(1):35-43.

19. Ferron M, Hinoi E, Karsenty G, Ducy P. Osteocalcin differentially regulates beta cell and adipocyte gene expression and affects the development of metabolic diseases in wild-type mice. Proc Natl Acad Sci U S A. 2008;105(13):5266-5270.

20. Lee NK, Karsenty G. Reciprocal regulation of bone and energy metabolism. J Musculoskelet Neuronal Interact. 2008;8(4):351.

21. Lee NK, Sowa H, Hinoi E, Ferron M, Ahn JD, Confavreux C, Dacquin R, Mee PJ, McKee MD, Jung DY, Zhang Z, Kim JK, Mauvais-Jarvis F, Ducy P, Karsenty G. Endocrine regulation of energy metabolism by the skeleton. Cell. 2007;130(3):456-469.

22. Yadav VK, Ryu JH, Suda N, Tanaka KF, Gingrich JA, Schutz G, Glorieux FH, Chiang CY, Zajac JD, Insogna KL, Mann JJ, Hen R, Ducy P, Karsenty G. Lrp5 controls bone formation by inhibiting serotonin synthesis in the duodenum. Cell. 2008;135(5):825-837.

23. Albala C, Yanez M, Devoto E, Sostin C, Zeballos L, Santos JL. Obesity as a protective factor for postmenopausal osteoporosis. Int J Obes Relat Metab Disord. 1996;20(11):1027-1032.

24. Felson DT, Zhang Y, Hannan MT, Anderson JJ. Effects of weight and body mass index on bone mineral density in men and women: the Framingham study. J Bone Miner Res. 1993;8(5):567-573.

25. Migliaccio S, Greco EA, Fornari R, Donini LM, Lenzi A. Is obesity in women protective against osteoporosis? Diabetes Metab Syndr Obes. 2011;4:273-282.

26. Zhao LJ, Liu YJ, Liu PY, Hamilton J, Recker RR, Deng HW. Relationship of obesity with osteoporosis. J Clin Endocrinol Metab. 2007;92(5):1640-1646.

27. Bredella MA, Torriani M, Ghomi RH, Thomas BJ, Brick DJ, Gerweck AV, Harrington LM, Breggia A, Rosen CJ, Miller KK. Determinants of bone mineral density in obese premenopausal women. Bone. 2011;48(4):748-754.

28. Bredella MA, Torriani M, Ghomi RH, Thomas BJ, Brick DJ, Gerweck AV, Rosen CJ, Klibanski A, Miller KK. Vertebral bone marrow fat is positively associated with visceral fat and inversely associated with IGF-1 in obese women. Obesity (Silver Spring). 2011;19(1):49-53.

29. Compston JE, Watts NB, Chapurlat R, Cooper C, Boonen S, Greenspan S, Pfeilschifter J, Silverman S, Diez-Perez A, Lindsay R, Saag KG, Netelenbos JC, Gehlbach S, Hooven FH, Flahive J, Adachi JD, Rossini M, Lacroix AZ, Roux C, Sambrook PN, Siris ES. Obesity is not protective against fracture in postmenopausal women: GLOW. Am J Med. 2011;124(11):1043-1050.

30. Sheu Y, Cauley JA. The role of bone marrow and visceral fat on bone metabolism. Curr Osteoporos Rep. 2011;9(2):67-75.

31. Nuttall ME, Gimble JM. Controlling the balance between osteoblastogenesis and adipogenesis and the consequent therapeutic implications. Curr Opin Pharmacol. 2004;4(3):290-294.

32. Elabd C, Basillais A, Beaupied H, Breuil V, Wagner N, Scheideler M, Zaragosi LE, Massiera F, Lemichez E, Trajanoski Z, Carle G, Euller-Ziegler L, Ailhaud G, Benhamou CL, Dani C, Amri EZ. Oxytocin controls differentiation of human mesenchymal stem cells and reverses osteoporosis. Stem Cells. 2008;26(9):2399-2407.

33. Bouxsein ML, Boyd SK, Christiansen BA, Guldberg RE, Jepsen KJ, Muller R. Guidelines for assessment of bone microstructure in rodents using micro-computed tomography. J Bone Miner Res. 2010;25(7):1468-1486.

34. Dempster DW, Compston JE, Drezner MK, Glorieux FH, Kanis JA, Malluche H, Meunier PJ, Ott SM, Recker RR, Parfitt AM. Standardized nomenclature, symbols, and units for bone histomorphometry: a 2012 update of the report of the ASBMR Histomorphometry Nomenclature Committee. J Bone Miner Res. 2013;28(1):2-17.

35. Luu YK, Lublinsky S, Ozcivici E, Capilla E, Pessin JE, Rubin CT, Judex S. In vivo quantification of subcutaneous and visceral adiposity by micro-computed tomography in a small animal model. Med Eng Phys. 2009;31(1):34-41.

36. Most W, van der Wee-Pals L, Ederveen A, Papapoulos S, Lowik C. Ovariectomy and orchidectomy induce a transient increase in the osteoclastogenic potential of bone marrow cells in the mouse. Bone. 1997;20(1):27-30.

37. Nelson HD, Humphrey LL, Nygren P, Teutsch SM, Allan JD. Postmenopausal hormone replacement therapy: scientific review. Jama. 2002;288(7):872-881.

38. Girotra M, Rubin MR, Bilezikian JP. The use of parathyroid hormone in the treatment of osteoporosis. Rev Endocr Metab Disord. 2006;7(1-2):113-121.

39. Tamma R, Colaianni G, Zhu LL, DiBenedetto A, Greco G, Montemurro G, Patano N, Strippoli M, Vergari R, Mancini L, Colucci S, Grano M, Faccio R, Liu X, Li J, Usmani S,

Bachar M, Bab I, Nishimori K, Young LJ, Buettner C, Iqbal J, Sun L, Zaidi M, Zallone A. Oxytocin is an anabolic bone hormone. Proc Natl Acad Sci U S A. 2009;106(17):7149-7154.

40. Richard S, Zingg HH. The human oxytocin gene promoter is regulated by estrogens. J Biol Chem. 1990;265(11):6098-6103.

41. Nishimori K, Young LJ, Guo Q, Wang Z, Insel TR, Matzuk MM. Oxytocin is required for nursing but is not essential for parturition or reproductive behavior. Proc Natl Acad Sci U S A. 1996;93(21):11699-11704.

42. Ferguson JN, Young LJ, Hearn EF, Matzuk MM, Insel TR, Winslow JT. Social amnesia in mice lacking the oxytocin gene. Nat Genet. 2000;25(3):284-288.

43. Takayanagi Y, Yoshida M, Bielsky IF, Ross HE, Kawamata M, Onaka T, Yanagisawa T, Kimura T, Matzuk MM, Young LJ, Nishimori K. Pervasive social deficits, but normal parturition, in oxytocin receptor-deficient mice. Proc Natl Acad Sci U S A. 2005;102(44):16096-16101.

44. Takayanagi Y, Kasahara Y, Onaka T, Takahashi N, Kawada T, Nishimori K. Oxytocin receptor-deficient mice developed late-onset obesity. Neuroreport. 2008;19(9):951-955.

45. Colaianni G, Sun L, Di Benedetto A, Tamma R, Zhu LL, Cao J, Grano M, Yuen T, Colucci S, Cuscito C, Mancini L, Li J, Nishimori K, Bab I, Lee HJ, Iqbal J, Young WS, 3rd, Rosen C, Zallone A, Zaidi M. Bone marrow oxytocin mediates the anabolic action of estrogen on the skeleton. J Biol Chem. 2012;287(34):29159-29167.

46. Deblon N, Veyrat-Durebex C, Bourgoin L, Caillon A, Bussier AL, Petrosino S, Piscitelli F, Legros JJ, Geenen V, Foti M, Wahli W, Di Marzo V, Rohner-Jeanrenaud F. Mechanisms of the anti-obesity effects of oxytocin in diet-induced obese rats. PLoS ONE. 2011;6(9):e25565.

47. Maejima Y, Iwasaki Y, Yamahara Y, Kodaira M, Sedbazar U, Yada T. Peripheral oxytocin treatment ameliorates obesity by reducing food intake and visceral fat mass. Aging (Albany NY). 2011;3(12):1169-1177.

48. Morton GJ, Thatcher BS, Reidelberger RD, Ogimoto K, Wolden-Hanson T, Baskin DG, Schwartz MW, Blevins JE. Peripheral oxytocin suppresses food intake and causes weight loss in diet-induced obese rats. Am J Physiol Endocrinol Metab. 2012;302(1):E134-144.

49. Zhang G, Bai H, Zhang H, Dean C, Wu Q, Li J, Guariglia S, Meng Q, Cai D. Neuropeptide exocytosis involving synaptotagmin-4 and oxytocin in hypothalamic programming of body weight and energy balance. Neuron. 2011;69(3):523-535.

50. Zhang H, Wu C, Chen Q, Chen X, Xu Z, Wu J, Cai D. Treatment of obesity and diabetes using oxytocin or analogs in patients and mouse models. PLoS ONE. 2013;8(5):e61477.

51. Macotela Y, Emanuelli B, Mori MA, Gesta S, Schulz TJ, Tseng YH, Kahn CR. Intrinsic differences in adipocyte precursor cells from different white fat depots. Diabetes. 2012;61(7):1691-1699.

52. Butler AA, Kozak LP. A recurring problem with the analysis of energy expenditure in genetic models expressing lean and obese phenotypes. Diabetes. 2010;59(2):323-329.

53. Karsenty G, Ferron M. The contribution of bone to whole-organism physiology. Nature. 2012;481(7381):314-320.

Table

Table 1: Micro-computed tomography analysis of femora trabecular parameters.

Early Treatment					
Femora Trabecular Parameters	Sham Ve	OVX Ve	OVX OT 1mg/kg	OVX OT short treatment	OVX OT twice a week
Tb. Th. (µm)	76 ± 1	70 ± 1 (a)	73 ± 1	68 ± 1 (a)	73 ± 1
Tb. Sp. (µm)	307 ± 11	380 ± 1 (a)	342 ± 6 (a,b)	366 ± 13 (a)	360 ± 13 (a)
Tb. N. (1/mm)	1.6 ± 0.1	1.2 ± 0.1(a)	1.5 ± 0.1(b)	1.2 ± 0.1(a)	1.4 ± 0.1(b)
Late Treatment					
Femora Trabecular Parameters	Sham Ve	Sham OT 1mg/kg	OVX Ve	OVX OT 0.1 mg/kg	OVX OT 1 mg/kg
Tb. Th. (µm)	73 ± 1	70 ± 1	66 ± 1 (a)	70 ± 1 (b)	70 ± 1 (b)
Tb. Sp. (µm)	430 ±19	373 ± 11(a)	603 ±16(a)	480 ± 11 (b)	509 ± 23(b)
Tb. N. (1/mm)	0.9 ± 0.1	1.0 ± 0.1 (a)	0.7 ± 0.1 (a)	1.0 ± 0.1 (b)	0.9 ± 0.1 (b)

Control (Sham) and ovariectomized (OVX) mice were submitted to daily injections of oxytocin (OT) or vehicle (Ve) for 8 weeks starting either 2 weeks (early treatment) or 8 weeks post-surgery (late treatment). Detailed analysis of trabecular parameters was performed on the distal metaphysis of femora. Trabecular Thickness (Tb. Th.), Trabecular Spacing (Tb. Sp.) and Trabecular Number (Tb. N.) are reported in the Table 1. a: $p<0.05$ vs Sham Ve; b: $p<0.05$ vs OVX Ve. (n=6 to 12 mice per group) Data are represented as mean +/- SEM.

Figures and Legends

Figure 1: Effects of oxytocin on trabecular bone parameters, body weight and fat mass in ovariectomized mice. Sham and OVX mice were submitted to daily injections of oxytocin (OT) or vehicle (Ve) for 8 weeks starting either 2 weeks (early treatment, **a**) or 8 weeks post-surgery (late treatment, **b**). Analysis of the trabecular bone from distal femoral metaphysis in OVX and Sham mice treated with OT or Ve. Mice were daily injected according to early (**c**, **e** and **g**) or late (**d**, **f** and **h**) treatment. Alternative treatments were performed (i.e. 2 injections per week, 4 weeks of OT treatment followed by 4 weeks of vehicle injections or a lower dose of 0.1 mg/kg). Trabecular bone volume was measured (**c**, **d**). Body weight was measured during early (**e**) and late (**f**) treatment. The volume of white adipose tissue between lumbar vertebra 1 and the caudal vertebra 4 was measured (**g**, **h**). BV/TV: Bone Volume/Tissue Volume ratio (n=6 to 12 mice per group), data are represented as mean +/- SEM, a $p<0.05$ vs Sham Ve; b $p<0.05$ vs OVX Ve.

Figure 2 : Plasma levels of bone formation marker PINP (a, b), bone resorption marker CTX-I (c, d), adipose tissue marker leptin (e, f) in Sham and OVX mice following 8 weeks of OT or Ve in early (a, c and e) and late (b, d and f) treatment. (n= 8-12 mice per group), data are represented as mean +/- SEM, a $p<0.05$ vs Sham Ve; b $p<0.05$ vs OVX Ve.

Figure 3: OT treatment restores osteoclast and osteoblast numbers as well as bone remodeling markers expression. In vivo analysis of long bones from Sham and OVX mice that were treated or not with OT. Decalcified bone sections were stained for Tracp activity (**a**) and Osterix expression (**c**) to quantify the Osteoclast (arrow) and Osteoblast (arrowhead) numbers respectively. Quantifications were performed from the growth plate up to the mid-diaphysis of femora on both trabecular and cortical bone. Quantitative representations of the illustrations on the left are shown in the graphs on the right of each panel. Real-Time PCR was performed on RNA from humeri and the expression of osteoclastic (**b**), osteoblastic (**d**), and pro-osteoclastogenic markers (**e**, **f**) was

determined. (n=12 mice per group), data are represented as mean +/- SEM, a $p<0.05$ vs Sham Ve; b $p<0.05$ vs OVX Ve. (scale bar: 10 µm).

Figure 4: OT induces osteoclastogenesis in a RANKL-dependent manner through mesenchymal cells. Monocytes isolated from bone marrow of OVX mice were differentiated in vitro in the presence of M-CSF and RANKL (**a, b**) or using a co-culture protocol with mesenchymal ST2 cells (**c**-**f**). Differentiation was performed in the absence or the presence of 300 nM OT, and osteoclast markers expression was measured by real-time PCR (**a**, **c**) on day 8. Osteoclast differentiation was quantified following TRACP staining (**b**, **d**), representative illustrations are shown on the right of each graph. Expression of RANKL/OPG ratio in co-culture of ST2 cells with primary monocytes from OVX mice (**e**) is reported. Effect of increasing amounts of OPG on OT-induced osteoclast differentiation in co-culture experiments (**f**) is shown. Data are represented as mean +/- SEM, a $p<0.05$ for OT-treated cells versus control (scale bar: 10 µm).

Figure 5: Increase in lipid metabolism of OVX-OT treated mice. Experimental design (**a**): treatment was initiated 8 weeks after surgery and consisted of a daily injection with vehicle or OT (1mg/kg) in Sham and OVX mice. Cumulative food intake (kcal) (**b**), total locomotors activity (**c**), energy expenditure (kcal/hr/kg of lean body mass) (**d**) and respiratory exchange ratio (vCO_2/vO_2) (**e**) were measured at two time points in the same group (during the 3rd or the 10th week of the treatment (arrows in panel **a**). Averages of daily and nocturnal data are presented as histograms (**b**-**d**). An average value for RER during a 4-hour period is presented as a histogram at the time period indicated by a black line (panel **e**). (n=6 in each group). Data are represented as mean +/- SEM, a $p<0.05$ vs Sham Ve; b $p<0.05$ vs OVX Ve.

Figure 6: OT treatment reduces both intra-abdominal and subcutaneous adipose tissues, effects on adipocyte size. Quantification of intra-abdominal (**a**) and subcutaneous (**d**) adipose depots after 8 weeks of late treatment. Adipose tissue areas were measured at the L5 (lumbar vertebra 5)

section level (**a**, **d**). Adipocyte size was measured on histological sections of intra-abdominal (**b**, **c**) and subcutaneous (**e**, **f**) adipose tissues and average adipocyte diameter (**b**, **e**) as well as adipocyte distribution size (**c**, **f**) were determined. (n= 8 mice per group). Data are represented as mean +/- SEM, a $p<0.05$ vs Sham Ve; b $p<0.05$ vs OVX Ve (scale bar:100 µm).

Figure 7: In vitro effect of OT on adipogenesis of primary adipose precursor cells. Stromal-vascular fraction cells isolated from subcutaneous adipose tissues from OVX mice were induced to differentiate into adipocytes in the absence or the presence of 30 or 100 nM OT. Microphotographs of differentiated cells at day 10 (**a**) and real time PCR of adipocyte markers (**b**) were performed in triplicate. Data are represented as mean +/- SEM, a 2-tailed Student's t -test was performed for the two OT doses independently, a $p<0.05$ vs ctrl (scale bar: 200 µm).

SUPPLEMENTAL DATA

Supplemental Materials and Methods

Supplemental Figures and Legends

Supplemental Figure 1: In vivo analysis of Tracp during the 2 weeks following ovariectomy. Tracp staining on decalcified bone sections (**a**) and quantification (**b**). Real-Time PCR for Tracp expression on RNA from humeri of Sham and OVX mice 2 weeks after ovariectomy (n= 4 mice per group), data are represented as mean +/- SEM, a $p<0.05$ vs Sham at 2 weeks. (Scale bar 500 µm).

Supplemental Figure 2: Fat (a) and lean (b) mass weight determined using Echo-MRI methods during the OT treatment period. Data are represented as mean +/- SEM.

Supplemental Figure 3: Bone marrow adiposity. In vivo analysis of fabp4 mRNA expression (a) and bone marrow adipocytes (b) within femora of Sham-Ve, OVX-Ve and OVX-OT treated mice. (n= 8-12 mice per group), data are represented as mean +/- SEM, a $p<0.05$ vs Sham-Ve, b $p<0.05$ vs OVX-Ve. (Scale bar 500 µm).

Supplemental Figure 4: Oxytoxin treatment affects meal ultrastructure. 4 and 18 h cumulative food intake at the 3rd (**a**) and the 10th (**b**) week of treatment period. Meals size (**c**) and duration (**d**) at the 3rd week of treatment period.

Supplemental Figure 5: **Triglyceride and glycerol quantification.** Triglyceride levels were quantified in Liver extracts (**a**). Circulating glycerol (**b**) and triglyceride (**c**) levels were quantified in plasma of Sham and OVX mice treated or not with OT. Data are represented as mean +/- SEM, a $p<0.05$ vs Sham Ve.

Supplemental Figure 6: OT treatment improves the insulin resistance in OVX mice. Glucose Tolerance test: mice were injected intraperitoneally with glucose (1.5 g/kg) before (**a**, **b**) or after (**c**, **d**) the 8-week oxytocin treatment. Glucose (**a**, **c**) and insulin (**b**, **d**) concentrations were measured in plasma from Sham and OVX OT or vehicle treated mice. (AUC: area under the curve) (n=8 mice per group), data are represented as mean +/- SEM.

Supplemental Figure 7: Plasma levels of undercarboxylated over carboxylated (Glu/Gla) osteocalcin ratio (**a, b**) in Sham and OVX mice following 8 weeks of OT or Ve in early (**a**) and late (**b**) treatment. (n= 8-12 mice per group), data are represented as mean +/- SEM, a $p<0.05$ vs Sham Ve; b $p<0.05$ vs OVX Ve.

Supplemental Figure 8: **OT treatment reduces both intra-abdominal and subcutaneous adipose tissues, effects on adipocyte size following the early treatment protocol.** Quantification of intra-abdominal (**a**) and subcutaneous (**b**) adipose depots following 8 weeks of early treatment. Adipose tissue areas were measured at the L5 (lumbar vertebra 5) section level using micro-computed tomography. Adipocyte size was measured on histological sections of intra-abdominal (**c**) and subcutaneous (**d**) adipose tissues at the end of the treatment period and adipocytes distribution according to their size is reported (n= 8 mice per group), data are represented as mean +/- SEM, a $p<0.05$ vs Sham Ve; b $p<0.05$ vs OVX Ve

Supplemental Table 1: Sequence of primers used for gene expression analysis.

Supplemental Table 2: Micro-computed tomography analysis of L4 vertebra trabecular parameters. Control (Sham) and ovariectomized (OVX) mice were submitted to daily injections of oxytocin (OT)

or vehicle (Ve) for 8 weeks starting 8 weeks post-surgery (late treatment). Detailed analysis of trabecular parameters was performed on the 4th Lumbar vertebra (L4). Trabecular Thickness (Tb. Th.), Trabecular Spacing (Tb. Sp.) and Trabecular Number (Tb. N.) are reported in the Table 2. a: $p<0.05$ vs Sham Ve; b: $p<0.05$ vs OVX Ve. (n=6 to 12 mice per group) Data are represented as mean +/- SEM.

Abbreviations

αMEM: alpha Minimum Essential Medium Eagle; BMI: Body Mass Index; BV/TV: Bone Volume/Trabecular Volume ratio (%); Col1α1: Collagen Type 1, Alpha 1, CTR: Calcitonin Receptor; CTX-I: C-Telopeptide of type I collagen; DMEM: Dulbecco's Modified Eagle Medium; fabp4: fatty acid binding protein 4; Micro-CT: Micro-Computed Tomography; OPG: Osteoprotegerin; OT: Oxytocin; OTR: Oxytocin Receptor; OVX: Ovariectomized mouse; PINP: Procollagen type I N-terminal Propeptide; PTH: Parathyroid Hormone; PCR: Polymerase Chain Reaction; RANKL: Receptor Activator of NFκB Ligand; RER: Respiratory Exchange Ratio; TNFα: Tumor Necrosis Factor alpha; TracP: Tartrate-Resistant Acid Phosphatase; Ve: Vehicle.

Figure
Click here to download high resolution image

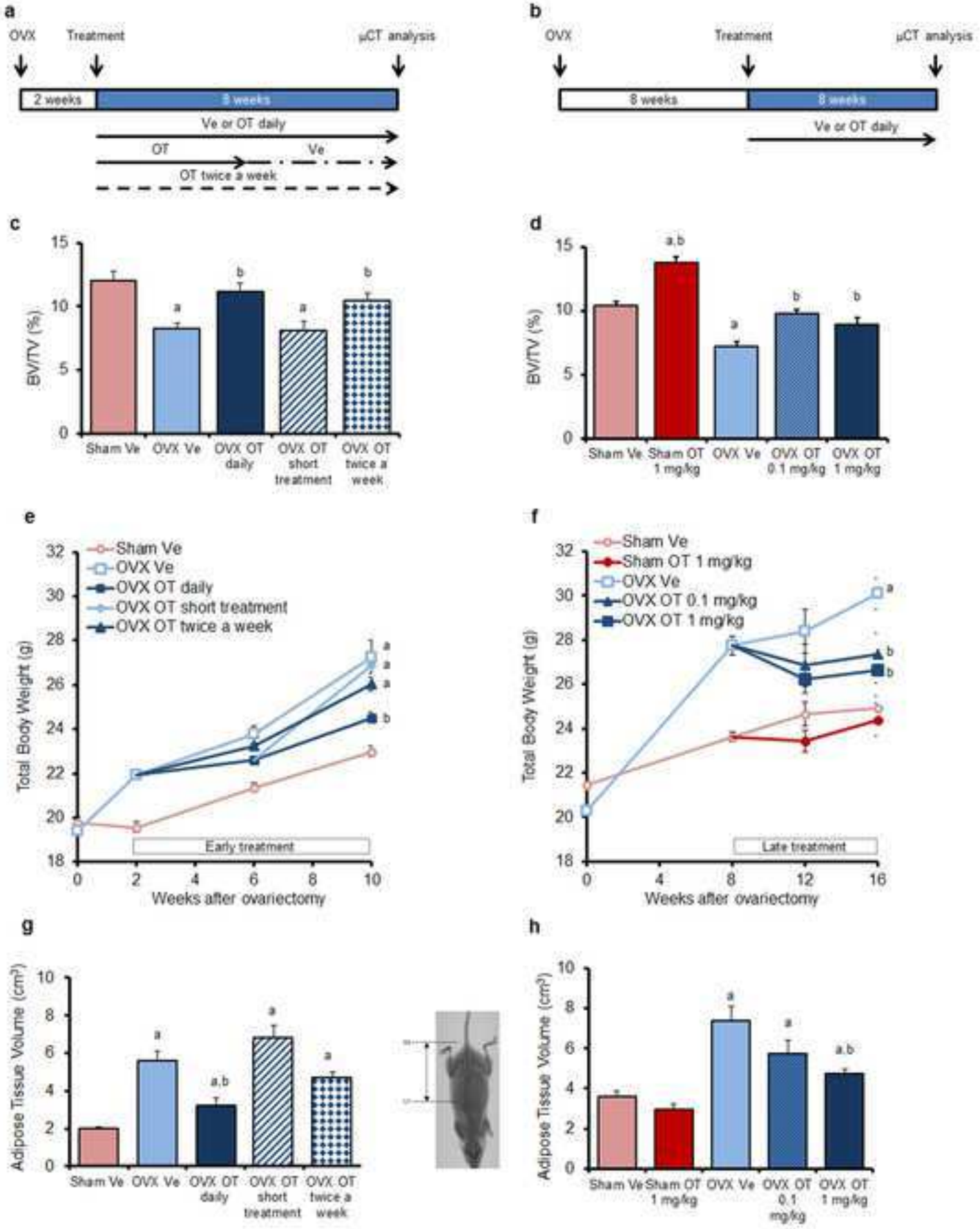

Figure
Click here to download high resolution image

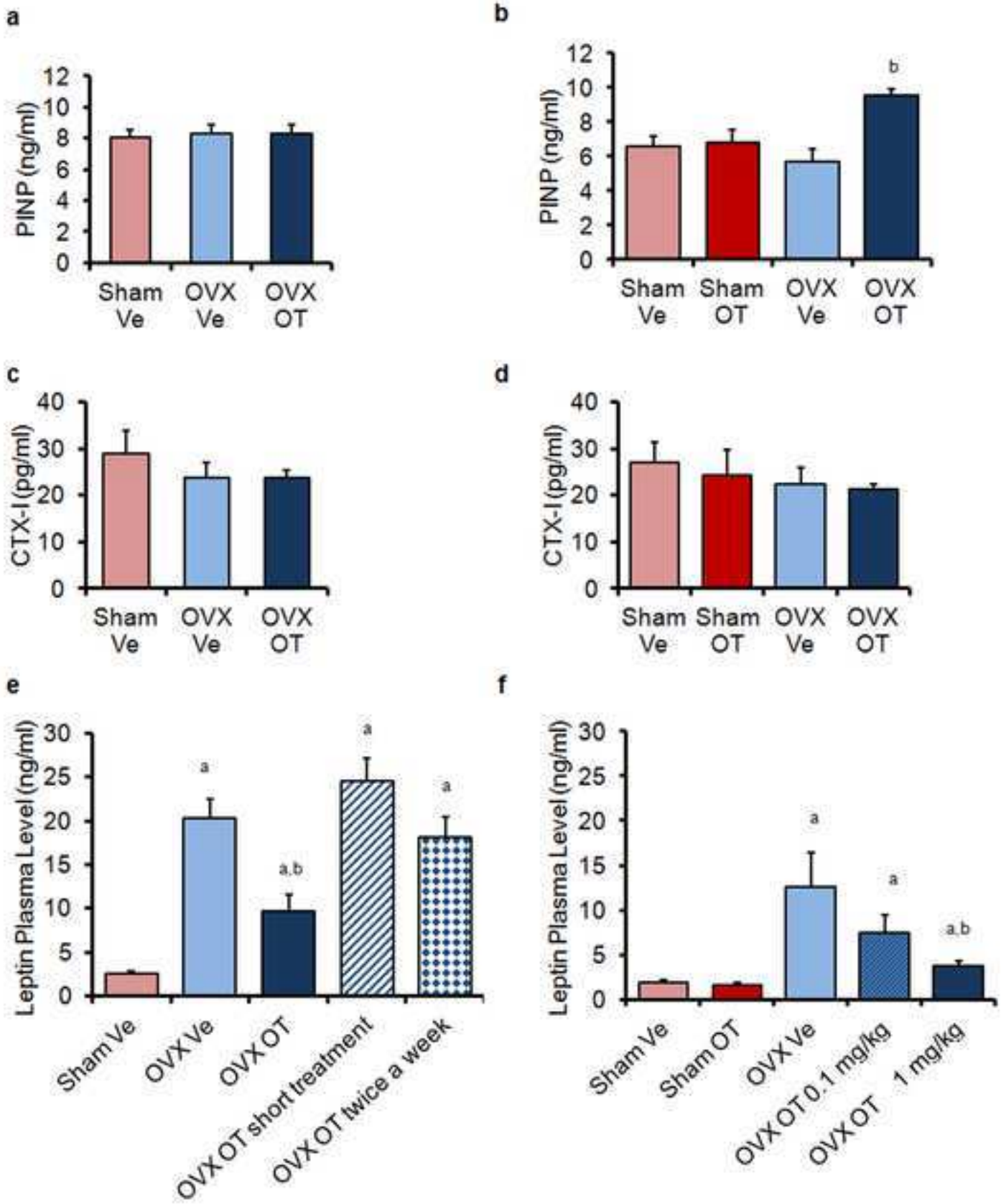

Figure
Click here to download high resolution image

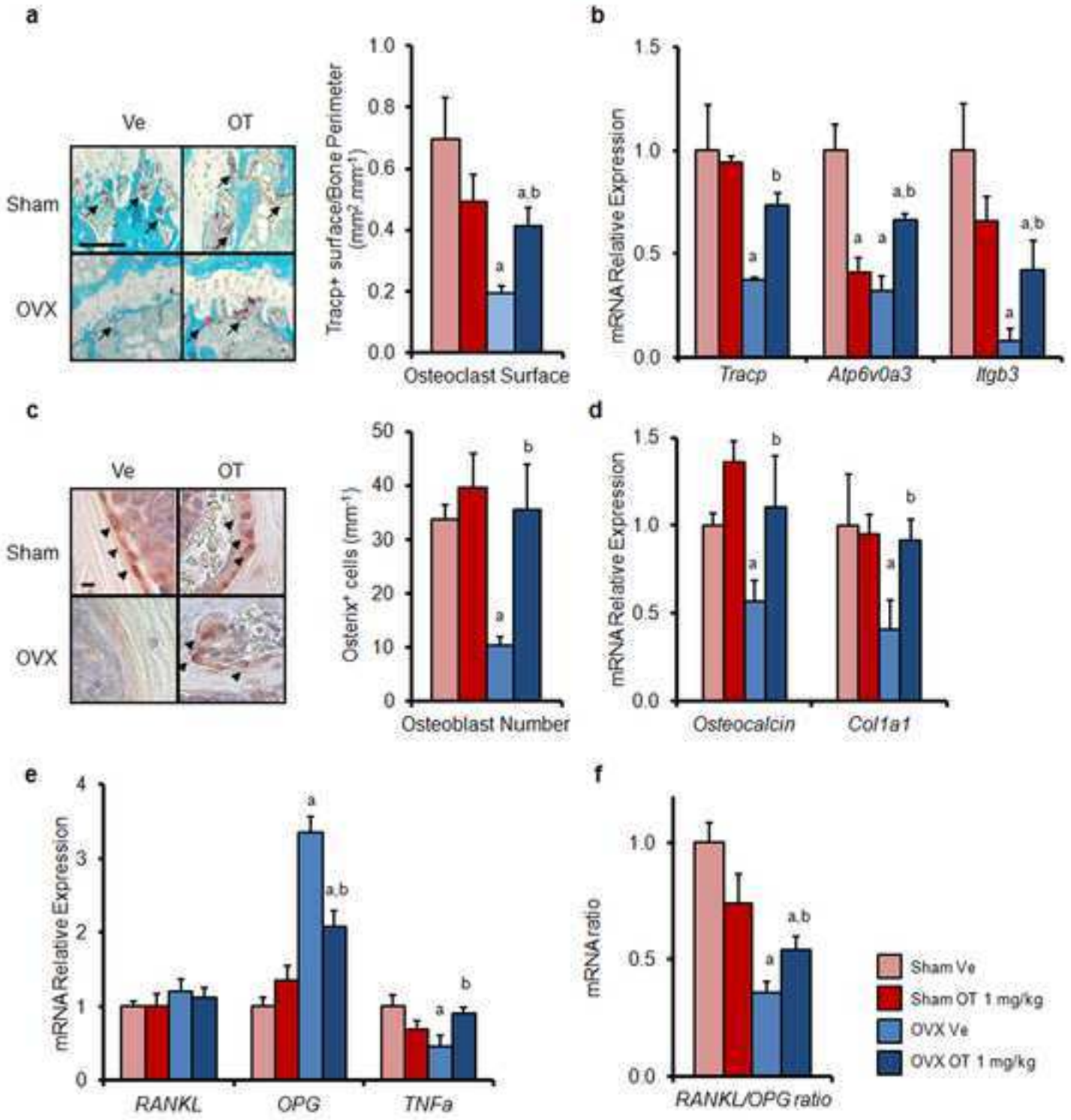

Figure
Click here to download high resolution image

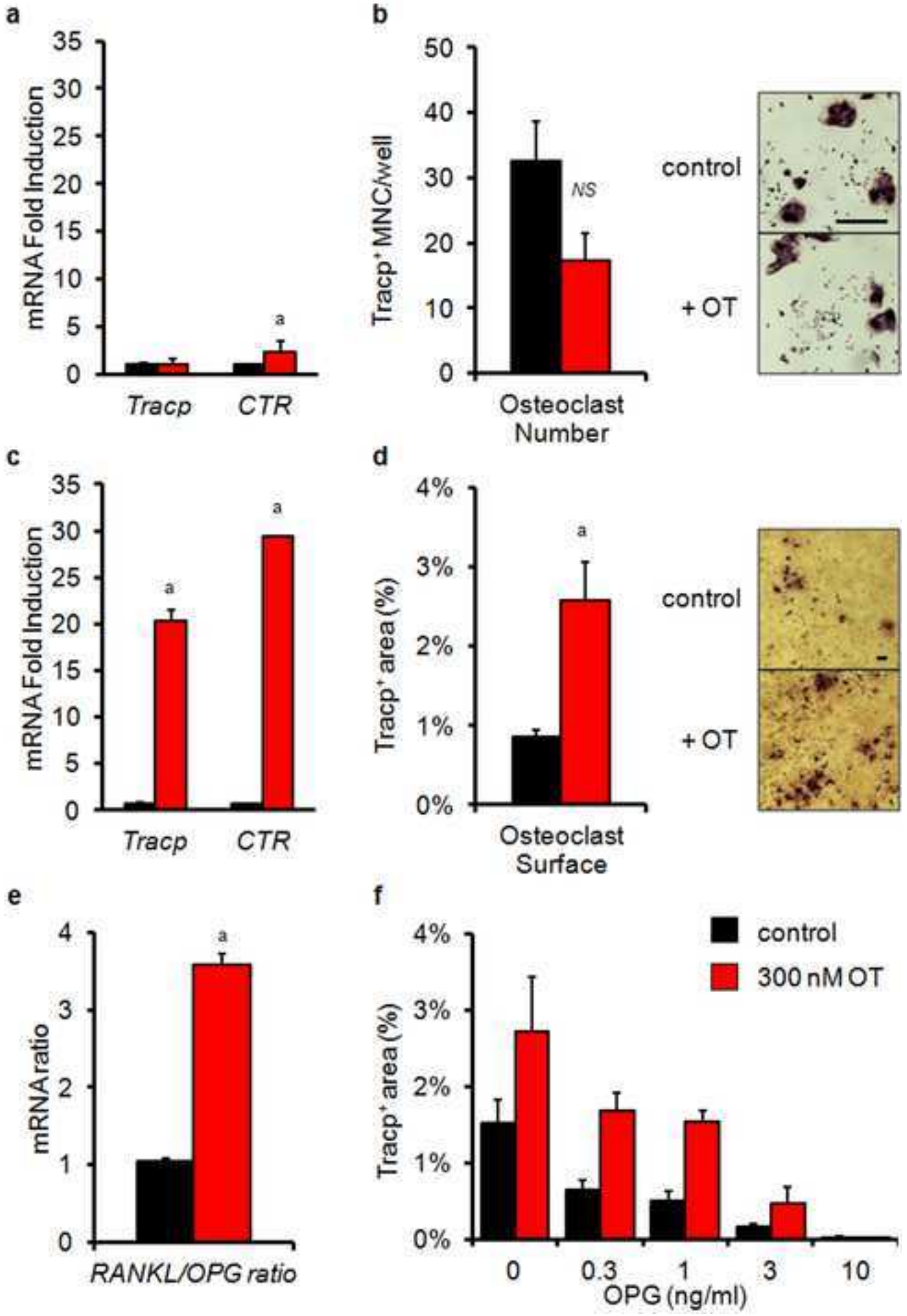

Figure 5
Click here to download high resolution image

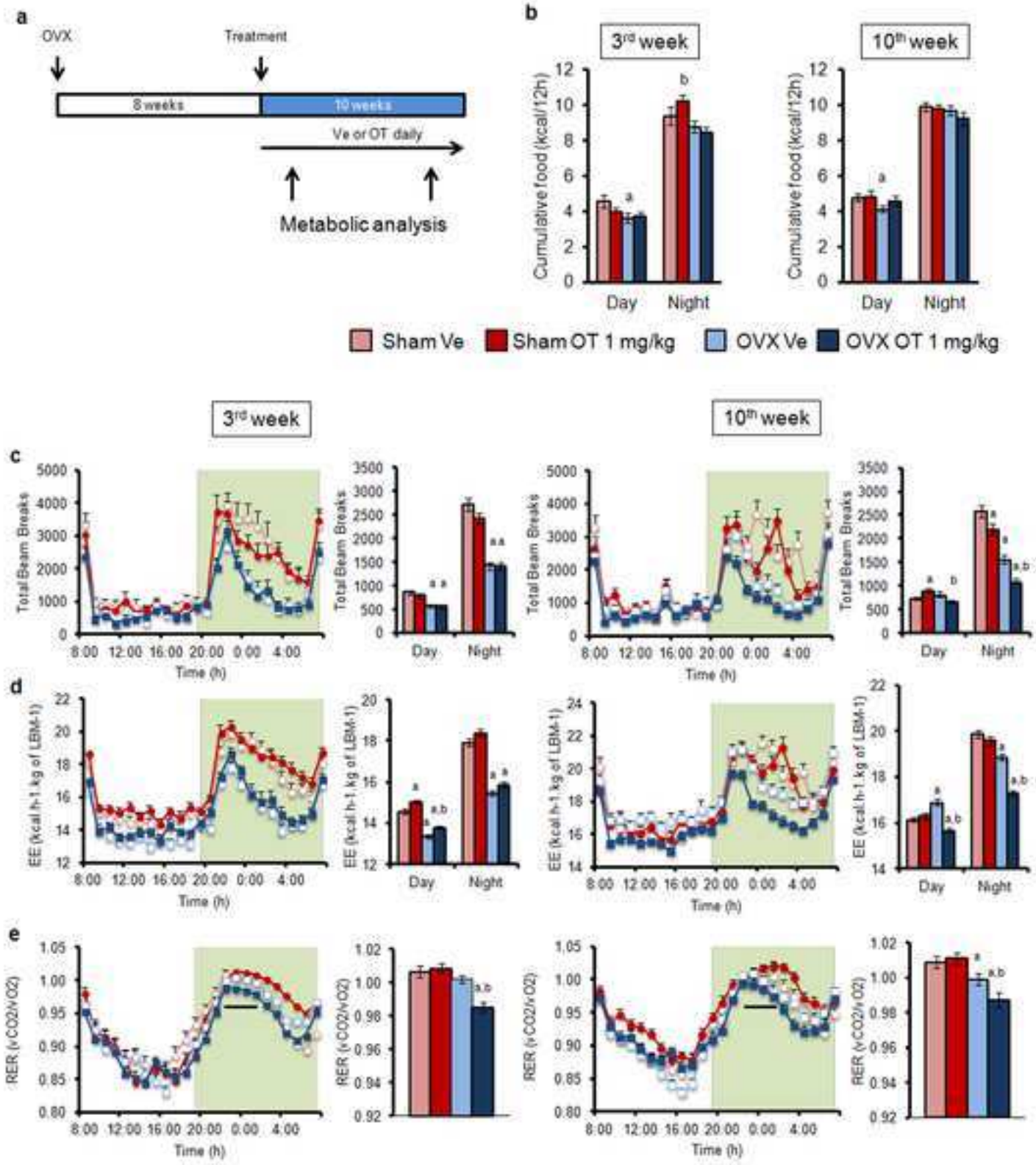

Figure 6
Click here to download high resolution image

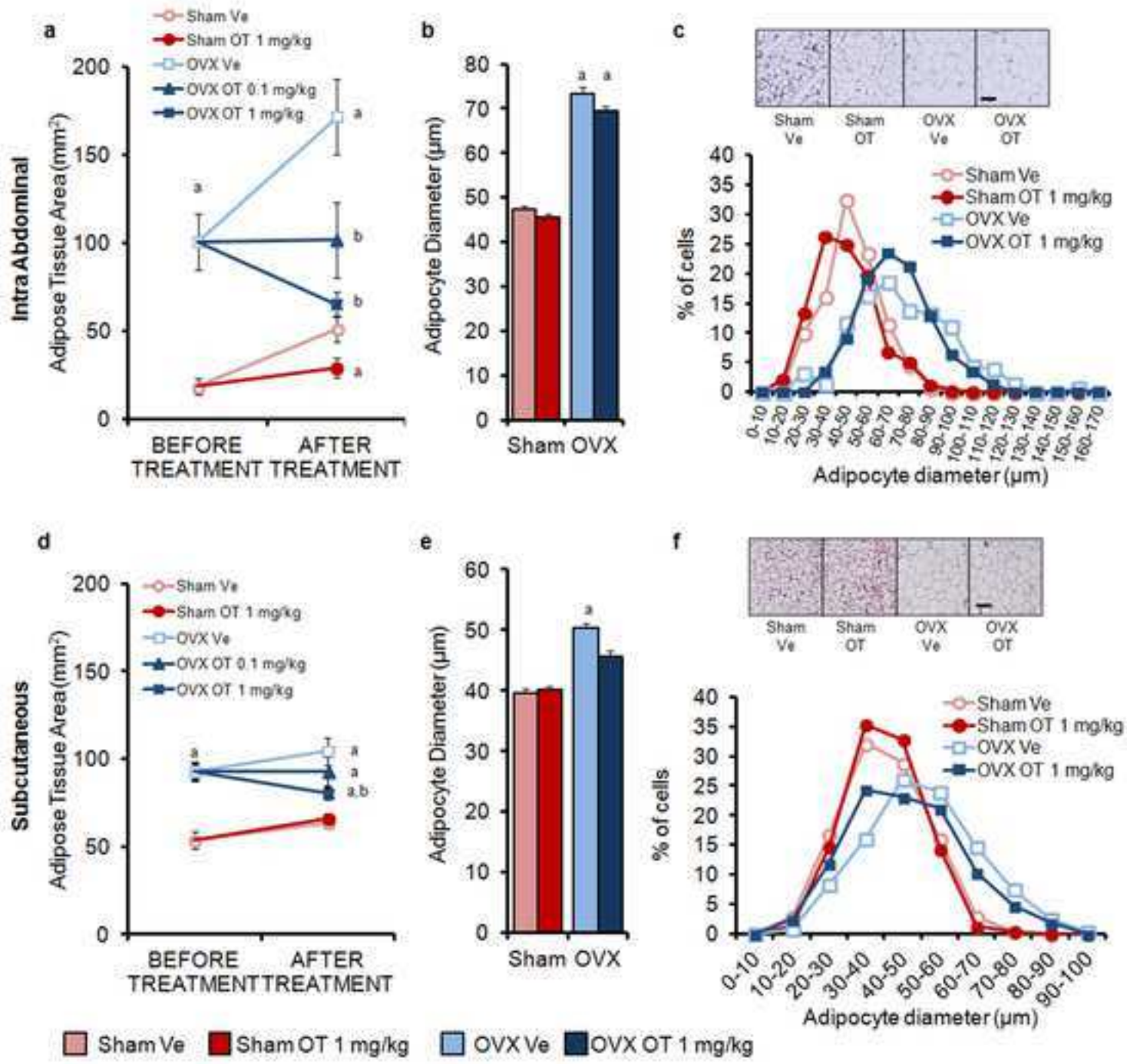

Figure 7
Click here to download high resolution image

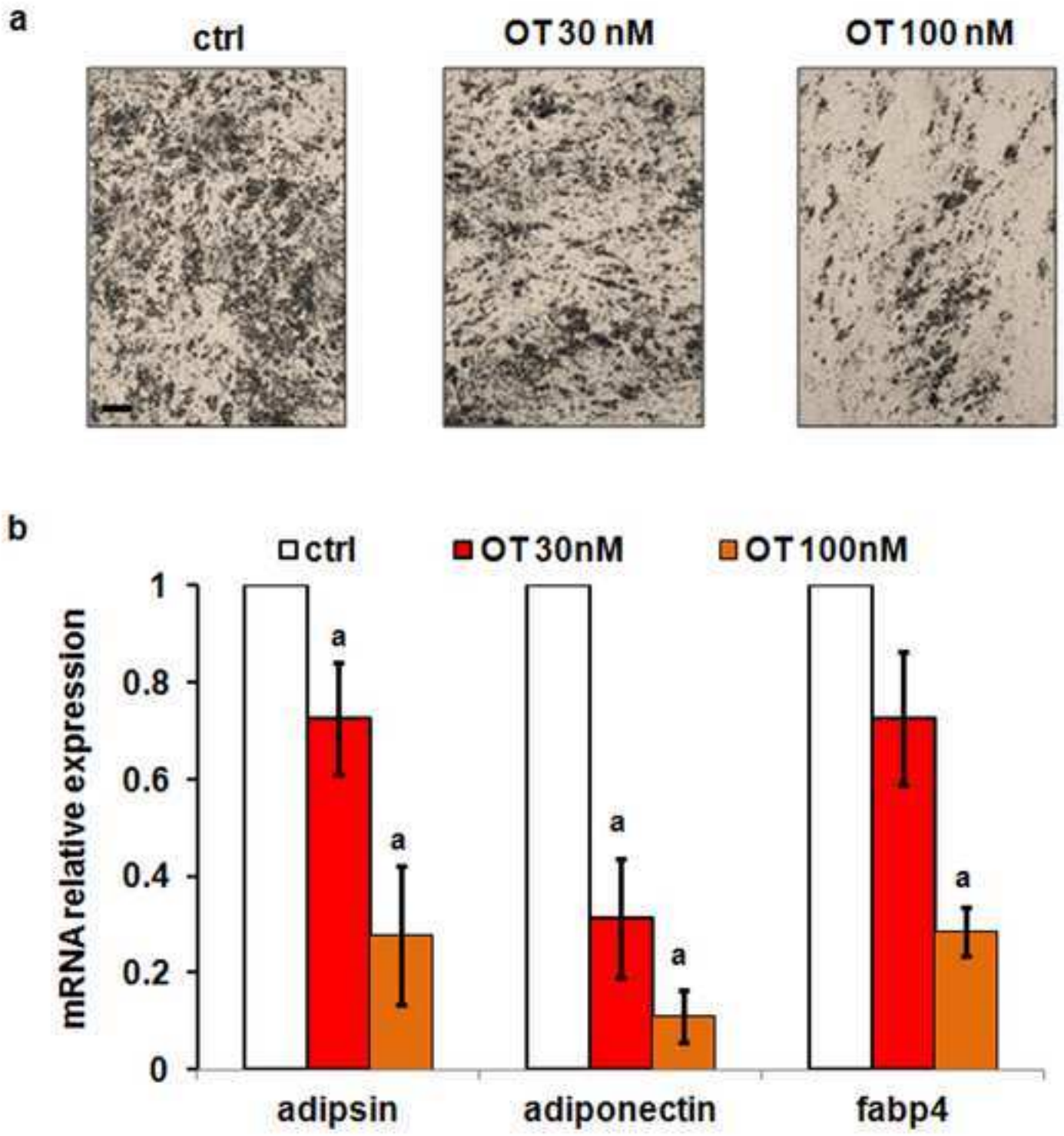

Antibody Table

Click here to download Table: Antibody Table.xlsx

Peptide/protein target	Antigen sequence (if known)	Name of Antibody
Osterix		Anti-Sp7 / Osterix antibody

Manufacturer, catalog #, and/or name of individual providing the antibody	**Species raised in; monoclonal or polyclonal**	**Dilution used**
Abcam #ab22552	Rabbit polyclonal	1/200